processes

MDPI

Article

Multivariate Monitoring and Evaluation of Dimensional Variability in Additive Manufacturing: A Comparative Study of EBM, FDM, and SLA

Abdulrahman M. Al-Ahmari [1,2], Moath Alatefi [1,2,*] and Wadea Ameen [3]

[1] Industrial Engineering Department, College of Engineering, King Saud University, P.O. Box 800, Riyadh 11421, Saudi Arabia; alahmari@ksu.edu.sa
[2] Raytheon Chair for Systems Engineering, King Saud University, P.O. Box 800, Riyadh 11421, Saudi Arabia
[3] Industrial Engineering Department, College of Engineering, Al Yamamah University, Riyadh 11512, Saudi Arabia; w_qaid@yu.edu.sa
* Correspondence: malatefi@ksu.edu.sa

Abstract

This study evaluates AM dimensional performance using multivariate quality control methods. Three-dimensionally printed products include multivariate correlated quality characteristics (QCs) that should be evaluated together. Furthermore, the same 3D-printed product can be produced by various additive manufacturing techniques, necessitating a comparative analysis to figure out which process provides superior quality. This study evaluates three AM processes—electron beam melting (EBM), fused deposition Modeling (FDM), and stereolithography (SLA)—to assess their performance in multivariate quality control. The research methodology focuses on monitoring, evaluating, and comparing these three AM processes. A standardized benchmark specimen is designed and fabricated using each AM process. Seven critical dimensional QCs were identified, and their specification limits were established based on ISO standards. Data collection was conducted using a high-precision measurement technique. This study used an improved Multivariate Exponentially Weighted Moving Average (MEWMA) control chart for process monitoring to detect deviations. The subsequent process evaluation used Multivariate Process Capability Indices (MPCIs) to assess conformance to specification limits. Then, a sensitivity study was conducted to assess the variability within each AM process. The findings identify the QC that contributes most to variation in each AM process and show clear differences in dimensional performance among EBM, SLA, and FDM, supporting process selection for precision applications.

Keywords: additive manufacturing; quality control; process capability; fused deposition modeling; stereolithography; electron beam melting

check for updates

Academic Editors: Salvador Tututi-Avila and George Z. Kyzas

Received: 18 October 2025
Revised: 18 November 2025
Accepted: 23 November 2025
Published: 26 November 2025

Citation: Al-Ahmari, A.M.; Alatefi, M.; Ameen, W. Multivariate Monitoring and Evaluation of Dimensional Variability in Additive Manufacturing: A Comparative Study of EBM, FDM, and SLA. *Processes* **2025**, *13*, 3825. https://doi.org/10.3390/pr13123825

Copyright: © 2025 by the authors. Licensee MDPI, Basel, Switzerland. This article is an open access article distributed under the terms and conditions of the Creative Commons Attribution (CC BY) license (https://creativecommons.org/licenses/by/4.0/).

1. Introduction

AM technologies—such as EBM, FDM, and SLA—have seen a rapid rise in usage in various applications [1,2]. Over the past decade, these technologies have evolved from simple prototyping tools to experiencing broader industrial adoption, including in commercial production methods [3]. However, concerns over how to consistently ensure the quality of 3D-printed components have grown more pressing as AM advances [4]. Traditional univariate quality control methods fail to capture the common variation among multiple variables in AM processes [5]. This has led to a growing interest in multivariate

process control tools, such as multivariate control charts and process capability measures, to monitor multiple QCs simultaneously [6].

Research on AM process monitoring has been somewhat limited, particularly in terms of assessing process stability [7,8]. Grigoriev et al. [7] present the relationship between the mechanical properties of 3D-printed parts (printed using FDM) and different polymer materials, including ABS, PLA, and PETG. Their study aimed to demonstrate how mechanical behavior varies based on the type of material and the percentage of infill. Similarly, Arwa et al. [9] assessed the dimensional accuracy of three types of inlays—3D-printed, milled, and conventionally fabricated. The findings revealed significant discrepancies among the printed parts, further highlighting the impact of manufacturing methods on final product accuracy. Building on the investigation of AM process quality, Shaharyar et al. [10] focused on characterizing process-induced volumetric defects that are difficult to eliminate because of the nature of the AM process. Their study employed X-ray computed tomography to examine the repeatability of scanning a similar laser powder bed-fused (L-PBF) AlSi10Mg material. A factorial experiment was conducted to analyze different levels of scan quality and better understand defect formation within AM-produced parts. Also, Peng et al. [11] explored the use of eddy current measurements as a novel approach for in situ real-time temperature monitoring during laser powder bed fusion (LPBF). The findings demonstrated effective temperature monitoring.

In many real applications, the three technologies can all be valid options, but each one comes with a different material class (metal, resin, polymer) and, therefore, different mechanical behavior, cost, and end-use suitability. The decision then is not only based on the application but also on the process that can achieve the required accuracy for this application, whether it is for prototyping, rapid tooling, or actual end-use manufacturing. By printing the same geometry and evaluating dimensional capability under a unified measurement and tolerance framework, we reveal how each process material combination performs when accuracy matters. This enables engineers to select the most appropriate technology based on evidence, not assumptions.

Despite growing evidence that multivariate approaches can offer deeper insight into AM process variations, relatively few studies have applied these methods to compare and evaluate different AM techniques under a unified framework [8,12]. This study aims to address the existing gaps in AM quality control by employing a multivariate approach to monitor and evaluate process performance. Multivariate control charts were used to track dimensional accuracy, and MPCIs were used to evaluate and compare the performance of FDM, SLA, and EBM. The sensitivity analysis quantitatively identifies which QCs have the largest impact on process variation, supporting targeted improvements in process planning and parameter selection. This research surveys the literature in Section 2, and Section 3 presents the research design. Section 4 details the methodology, Section 5 presents the results, Section 6 discusses the research findings, and, finally, Section 7 concludes the study.

2. Literature Review

AM has seen rapid growth in recent years, with techniques like FDM, SLA, and EBM becoming increasingly common in both research and industry [13–15]. These technologies offer unique advantages depending on the materials used and the specific application, which has led to a wide range of studies exploring their capabilities [16–18]. Researchers have given much attention to evaluating AM processes' mechanical performance and dimensional accuracy [19].

The EBM process, a widely used metal AM technique known for producing high-performance components [20–22], has demonstrated excellent physical and mechanical properties [1,23,24]. Only a limited number of researchers have focused on the quality

of metal AM [25]. Lee, Jungeon, et al. conducted a comprehensive review of numerical and experimental methods for monitoring quality in metal AM, comparing them with techniques used in traditional metal manufacturing [26]. Edwards also explored the mechanical properties of Ti-6Al-4V alloy samples printed using EBM. He found that increasing the bed temperature helped reduce residual stresses. However, this approach did not consider optimizing part quality [27]. Furthermore, Celia et al. [28] assessed the mechanical properties of Ti-6Al-4V hip implant EBM parts. Their study concluded that combining AM with heat treatments significantly enhances the suitability of Ti-6Al-4V for orthopedic implants. Moazzen et al. [29] also revealed similar results.

Moreover, the FDM process has been extensively studied in the literature, particularly regarding its design and modeling [30,31]. Notable previous studies in this area include the works of Bellini et al. [32] and Agarwala et al. [33], which analyzed power consumption during printing and variations in filament diameter as it exits the nozzle. Additionally, the effect of nozzle positioning on the quality and dimensional accuracy of 3D-printed parts has been investigated [34].

According to Redwood et al. [35], vat polymerization (such as SLA) is one of the major categories of AM techniques. SLA involves using ultraviolet (UV) radiation to solidify the starting material. There are two main types of SLA devices—one utilizes mirrors to reflect UV light onto the material from above, while the other directs light from below [36]. Many researchers have studied the SLA process [4]. Huang [37] examined the four generations of SLA processes and provided a detailed discussion of the representative system configurations associated with each generation. The quality improvements of SLA products begin with controlling the process using multivariate control charts. There have been attempts to monitor the SLA process [38,39]; however, these studies used a univariate control chart for each characteristic. An evaluation of the SLA process has also been conducted by Zhao et al. [40] to measure the process capability in terms of specific characteristics, such as dimensional accuracy and mechanical properties. Many optimization tools have been used to improve the SLA process, such as parametric optimization [41], response surface methodology [42], multiobjective optimization [43], and Neural Network Optimization [44].

Recent studies have underscored the significance of process understanding and data-driven modeling in additive manufacturing. Research on AI-driven hybrid optimization for PLA-CF composites indicates that machine learning models can precisely predict key quality metrics, including surface roughness and kerf width, by establishing correlations between process parameters and dimensional outcomes [45]. Similarly, the review titled Advances in 3D Printing of Thermoplastic Polymer Composites highlights how process physics, thermal characteristics, and layer-by-layer mechanisms influence dimensional accuracy in polymer additive manufacturing [46]. Together, these studies highlight the importance of characterizing additive manufacturing processes to understand how process parameters affect dimensional accuracy, thereby reinforcing the foundation of the current research.

Considering the amount of research on EBM, FDM, and SLA, most studies still focus on improving univariate process parameters, materials, and design considerations in isolation [4,47–51]. Only considering one variable at a time [52,53] can lead one to miss important interactions between different QCs that affect final part quality. There is still very limited work comparing these technologies side by side using multivariate methods, which can provide a more complete picture of dimensional consistency. This gap highlights the need for systematic methods for monitoring, evaluating, and comparing different AM processes using multivariate techniques.

3. Research Design

The key stages involved in assessing multivariate quality control for AM processes are shown in Figure 1, with a focus on dimensional features. The process begins with the part design phase, which serves as the starting point for producing a part that meets specific dimensional criteria. Central to the analysis are the critical QCs of the designed part. These QCs are essential dimensional features that require rigorous monitoring to ensure the final product's quality and conformity to design specifications. The critical QCs include measurements such as Pin Diameter X and Pin Diameter Y, which denote the pin diameters along the X and Y axes, respectively. Additionally, Hole Diameter X and Hole Diameter Y measure the hole diameters in the corresponding directions, while the LF (lateral feature) Hole Diameter represents the diameter of the lateral hole in the part. The LF Square Width and LF Square Height refer to the width and height of lateral square features. Monitoring these dimensional QCs ensures that the manufactured parts achieve the desired accuracy and performance. The part manufacturing phase involves fabricating the designed part using different AM technologies, including EBM, FDM, and SLA apparatus. Each of these processes has unique characteristics that influence the precision and variability of the dimensional features of the final product. The primary objective is to monitor, evaluate, and compare the multivariate QCs of AM processes. This involves analyzing how well EBM, FDM, and SLA maintain the critical dimensional features outlined in the QCs. This analysis supports informed decisions on process selection and optimization to enhance the quality of parts produced through AM.

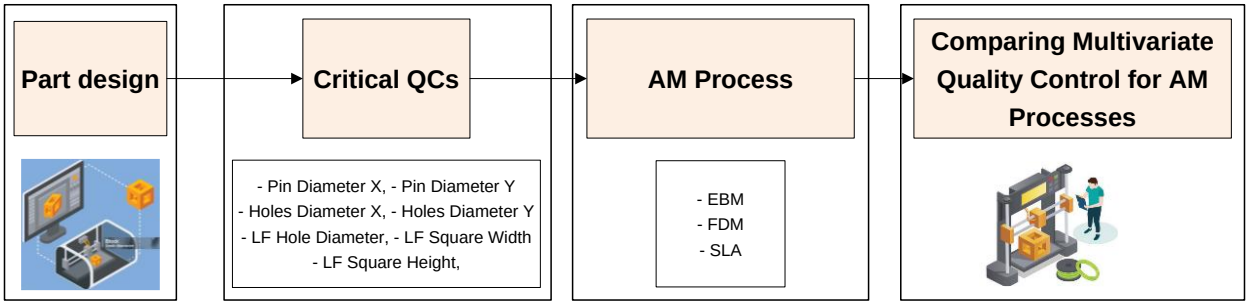


Figure 1. Stages involved in assessing multivariate quality control for AM processes.

4. Research Methodology

The research methodology in Figure 2 presents a structured approach to evaluating AM processes, specifically EBM, FDM, and SLA. It begins with selecting an AM process, followed by identifying the critical QCs and their specification limits. In the process monitoring phase, the multivariate control chart is selected, optimized, and drawn to assess process stability. If the process is unstable, it loops back to monitoring for further refinement. If stability is achieved, the methodology proceeds to process evaluation, where data and specifications are standardized, correlation matrices are computed, and large samples are simulated to estimate the percent of nonconforming (PNC) samples. The Multivariate Process Capability Index (PCI) is then calculated to assess performance. Finally, the sensitivity analysis phase is conducted, where variation causes are analyzed. This structured methodology ensures effective process monitoring, capability assessment, and quality improvement in AM systems.

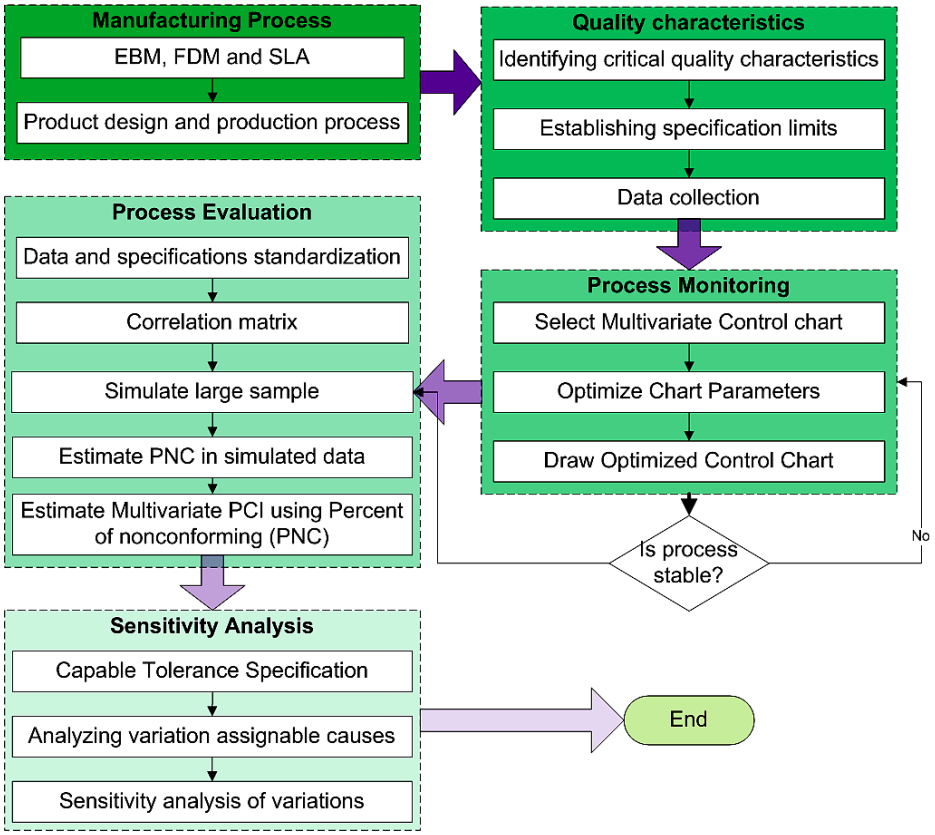


Figure 2. Generic methodology of multivariate evaluation of dimensional variability of AM processes.

4.1. Processes and Part Design and Production

To achieve the intended objectives of assessing of dimensional accuracy of EBM, FDM, and SLA processes, the benchmarking specimen from Moylan et al. [54], depicted in Figure 3, was selected. The selection of this part was justified by its diverse features, which comprehensively represent various Geometric tolerancing and dimensioning characteristics. Additionally, it includes lateral features, mini features, and staircases, all integrated into a compact design.

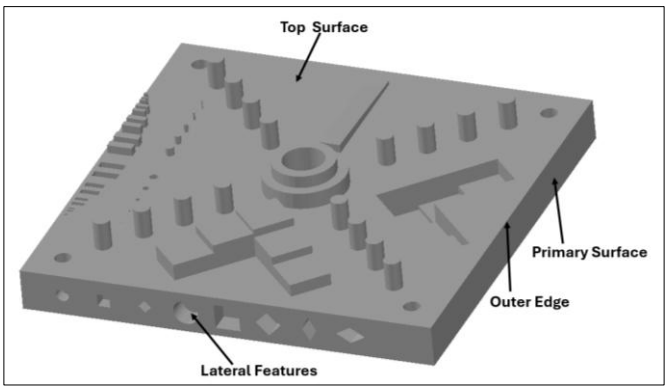


Figure 3. Benchmarking specimen [54].

In this study, three AM processes were evaluated using industrial-grade equipment. The Dimension Elite 3D printer, an FDM system, shown in Figure 4a, sourced from Stratasys Ltd. (Eden Prairie, MN, USA), was used to fabricate the polymer specimens. The Ultra 3SP 3D printer, an SLA system, in Figure 4b, obtained from EnvisionTEC GmbH (Gladbeck, Germany), was used to produce the resin-based parts. For metal fabrication,

the ARCAM A2 machine, an EBM system, in Figure 4c, manufactured by Arcam AB (Gothenburg, Sweden), was employed.



Figure 4. Additive manufacturing systems: (**a**) Dimension Elite 3D printer, (**b**) Ultra 3SP 3D printer, and (**c**) ARCAM A2 EBM machine.

To guarantee a reliable and equitable comparative analysis, the build orientation of the standardized specimen was meticulously regulated and maintained uniformly across all three additive manufacturing processes (EBM, FDM, and SLA). Specifically, the specimen was manufactured with a horizontal orientation, with the build vector extending from the base of the part upward along the *Z* axis, as illustrated in Figure 3. This standardization reduces the impact of intrinsic process anisotropy and layer effects on the resulting dimensions. No support structures are incorporated into the specimens during processing by the tree AM systems, and this is due to the absence of overhang features.

The parameters were selected based on a literature review. Each part was manufactured using the most suitable processing parameters for the respective material within the AM system. The FDM printer used in this study supports two layer thickness options and three model interior densities. In the SLA system, the only adjustable parameter was layer thickness, as the software provided limited accessibility for parameter modifications. Table 1 presents the processing parameters for each machine.

Table 1. Manufacturing parameters for FDM, SLA, and EBM AM processes.

AM Processes	FDM	SLA	EBM
Operational parameters and settings	Layer thickness 0.254 mm	Penetration depth 0.025 mm	Layer resolution 0.05 mm
			Beam current 19 mA
	Interior model solid (100%)	Acrylonitrile butadiene styrene as the material type	Scanning speed: 2200 mm/s
			Temperature of power bed 1100 °C
	Materials: Acrylonitrile butadiene styrene		Acceleration voltage of 60 kV
		Liquid material state	Line offset: 0.2 mm
			Line energy 0.54 J/mm
	Solid material state		Energy per unit area 2.71 J/mm^2
			Material: Gamma titanium aluminide
			Powder material state

Figure 5 illustrates the three different parts produced by these systems. Different layer thicknesses used for FDM, SLA, and EBM (Table 1) were selected and optimized to achieve optimal performance for each specific process and material. Due to the fundamental operational variations and machine limitations unique to each technology (e.g., beam physics versus photopolymerization), a direct numerical standardization of layer thickness across all three processes was not attainable. This guaranteed that the maximum potential of each process could be evaluated.

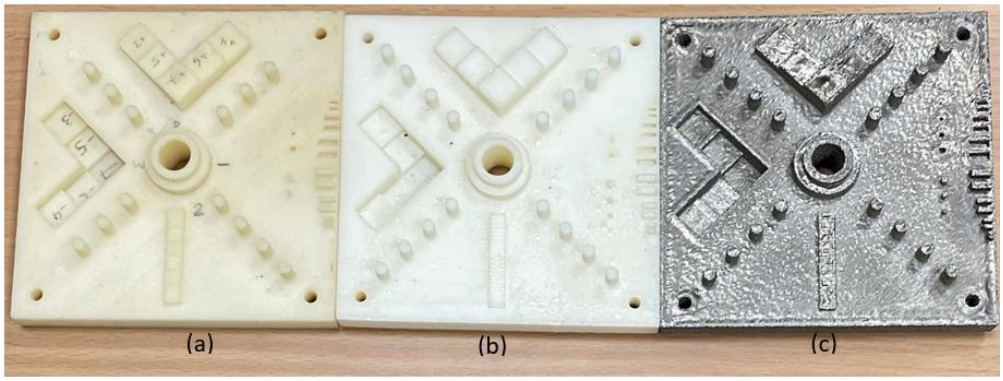


Figure 5. Parts produced by AM systems: (**a**) FDM, (**b**) SLA, and (**c**) EBM.

For each AM process, 30 specimens were produced (one part at a time) and measured, giving a sample size of $n = 30$ per process. This sample size is consistent with typical AM capability studies and provides adequate data for estimating the mean vector, covariance structure, and multivariate capability index.

4.2. Data Collection

A coordinate measurement machine (CMM) was chosen to conduct the measurements due to its remarkable precision. In this study, a bridge-type CMM equipped with a touch probe, as depicted in Figure 6, was utilized. Each feature and its corresponding dimensions were measured three times, and then the mean of each feature measurement was estimated. To determine the diameters of various features, at least six points were evenly distributed over 360°. The part was secured on the CMM, as shown in Figure 6, for assessing the top surface and lateral features, respectively. This straightforward fixture setup minimized measurement uncertainty.



Figure 6. Coordinate-measuring machine.

4.3. Nominal and Specification Limits

Specification limits were set to assess whether each AM process can meet the required dimensional accuracy. Specification limits define the acceptable range within which each quality characteristic (QC) must fall to be considered compliant with design requirements. In AM processes, these limits are often based on industry standards that dictate general tolerances.

Two types of limits are used in this study. The ISO-based specification limits, which represent the design tolerances according to ISO 2768 [55], and the natural process limits, which represent the intrinsic process spread. For the capability analysis, natural limits are presented as a separate category to provide a baseline of inherent process capability, enabling comparison with ISO-defined requirements.

ISO 2768 was selected as a neutral, geometry-based tolerance reference to enable consistent evaluation across the three AM technologies. The benchmark specimen used in this study is not tied to a customer-specific application; therefore, a general tolerance standard is appropriate. Although several AM-specific standards exist (ISO/ASTM 52900 series), they do not define general dimensional tolerance classes for arbitrary geometries. ISO 2768 is commonly adopted in AM benchmarking studies for this purpose, providing a uniform baseline for comparing dimensional variability among different processes [39].

The ISO 2768 standard is a widely recognized guideline that categorizes tolerances into four classes: Fine, Medium, Coarse, and Very Coarse. The tolerance class for each dimensional characteristic was selected based on its nominal size range, ensuring consistent scaling of tolerance bands across the three AM processes. Because MPCI expresses capability relative to the specified tolerance zone, comparisons across tolerance classes and processes are inherently normalized. The analysis is descriptive, and no inferential hypothesis testing was performed; therefore, no multiple-comparison adjustment was required.

In additive manufacturing, the selection of specification limits must account for the inherent variability associated with different processes. The choice of tolerance class—ranging from tighter tolerances in the Fine category to broader tolerances in the Very Coarse category—depends on the intended application of the part and its dimensional precision requirements. This systematic approach ensures that the produced components conform to established standards and maintain functional reliability.

Furthermore, this study investigated three AM processes—EBM, FDM, and SLA—under controlled operating conditions. Standardized test specimens were fabricated for each process, with multiple replicates produced to capture the inherent variability of each method [56]. Several critical dimensions were selected based on functional relevance (e.g., thickness, length, and hole diameter). All dimensions were measured using high-precision equipment, and reliability was verified through a measurement system analysis (MSA) prior to data collection [8].

Natural tolerances, sometimes referred to as natural specification limits, are derived directly from the process data and intended to capture the range within which the vast majority (typically 99.7%) of in-control observations fall [6]. They differ from externally imposed engineering tolerances by reflecting the process's current performance boundaries. In this study, the natural specification limits were determined through the following equation for each measured dimension:

$$\textit{Natural Specification limits} = \overline{X} \pm 3\sigma \quad (1)$$

where $\overline{X}$ is the sample mean, and σ is the standard deviation.

4.4. Process Monitoring

This work represents a Phase I study. Samples are not time-ordered but collected under controlled conditions. Control charts were applied only to verify that the process was in-control, as capability analysis cannot be conducted on unstable processes. The purpose is to estimate the in-control process parameters and evaluate the multivariate capability of each AM process rather than to perform ongoing monitoring.

MEWMA works perfectly with multivariate QCs of AM processes because of its ability to detect small shifts in the process. The chart, established by Lowry et al. [57], first transfers each QC to standard values using the following equation (Equation (2)):

$$\begin{gathered} z_i = \lambda x_i + (1-\lambda) z_{i-1}, \\ i = 1,\ 2,\ \ldots,\ n, \end{gathered} \tag{2}$$

The number of multivariate QCs is n, where λ is the chart constant, taken to be between 0 and 1; $z_0 = \mu_i$ (*mean of ith QC*). To monitor the multivariate QCs of the process simultaneously, the multivariate value of each simple is calculated using the following formula:

$$T^2 = z_i{}' \, \Sigma_{z_i}{}^{-1} \, z_i \tag{3}$$

The MEWMA has an upper control limit h_4, which is chosen from previously simulated values based on the desired average run length (*ARL*). The process is considered unstable if $T^2 => h_4$.

ARL measures the average number of samples taken before a control chart signals an out-of-control condition. Σ_{Z_i} denotes the covariance matrix of Z_i:

$$\Sigma_{Z_i} = \frac{\lambda \times \left(1 - (1-\lambda)^{2i}\right)}{2-\lambda} \times \Sigma, \tag{4}$$

Σ (covariance matrix) is estimated for multivariate QC data. However, choosing the right chart parameters is necessary to optimize the MEWMA chart. Thus, the suggested approach uses Monte Carlo simulation to find the ideal MEWMA parameters (h_4 and λ) so that the ARL is equal to 370, a widely used standard in the literature [6,58]. When the process is under control, this goal is equivalent to the probability ($p = 0.0027$) that a point will surpass the $\mu \pm 3\sigma$ controls. Thus, $ARL = 1/p = 1/0.0027 = 370$ is the anticipated number of samples before a false alert signal.

Therefore, the MEWMA control chart optimization algorithm proposed by Moath et al. [8], shown in Figure 7, was used select the best parameters of MEWMA. The algorithm initially examines the normality assumption of the multivariate QC data. The non-normal data are then transferred using root transformation.

Optimizing MEWMA control chart parameters is based on simulating large simples using the multivariate data parameters (mean and covariance).

The MEWMA design parameters (h_4 and λ) were tuned using Monte Carlo simulation to achieve a nominal in-control average run length of $ARL0 = 370$. For each candidate pair, $N = 1{,}000{,}000$ independent in-control sequences were simulated, and the *ARL* estimate was computed as the mean number of samples until the first signal. A fixed random seed was used to ensure reproducibility. The number of replications, N, was chosen to be large enough so that the Monte Carlo standard error of the *ARL* estimate was small compared with the target *ARL*. Convergence was checked by increasing N and confirming that the *ARL* estimate changed by less than a few units.

The simulated data are transformed to MEWMA data using a given initial parameters, before being drawn against the chart control limit to identify when an out-of-control

signal appears (*ARL*). If the calculated *ARL* equals 370, the algorithm terminates, and the optimal MEWMA parameters are obtained. Otherwise, the algorithm continues by adjusting either λ or h_4. In practice, several runs of the algorithm are conducted using different h_4 values. For each fixed h_4, the smoothing constant λ is iteratively varied until the condition $ARL = 370$ is satisfied.

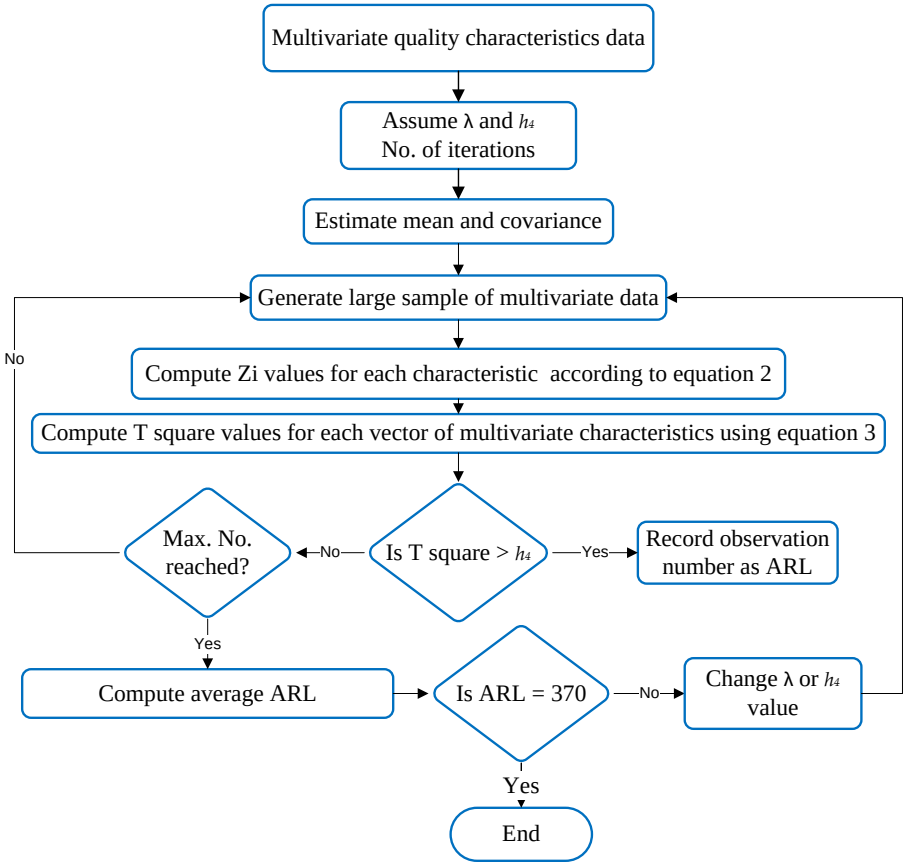


Figure 7. Algorithm for optimizing MEWMA parameters [8].

4.5. Process Evaluation

Evaluation of AM processes with multivariate QCs required the use of multivariate evaluation tools. Therefore, this research used the Multivariate Process Capability Index to measure the capability of the process to produce 3D-printed parts within the desired specification limits. The steps of the estimation algorithm are as follows [59]:

- The standard values of each QC are calculated using the following formula:

$$Z_i = \frac{Y_i - \hat{\mu}_{Y_i}}{\hat{\sigma}_{Y_i}};\ i = 1, 2, \ldots, p \tag{5}$$

Let Y_i denote the observed or transformed data for the *ith* QC, where p represents the total number of QCs. The estimated mean and standard deviation of Y_i are denoted by $\hat{\mu}_{Y_i}$ and $\hat{\sigma}_{Y_i}$, respectively. Furthermore, the specification limits for each QC are standardized with respect to their corresponding QC mean and standard deviation, ensuring consistency in the evaluation of process performance across different QCs.

- To ensure the steady state of the process, a large sample size is generated from a standard multivariate normal distribution, utilizing the standardized data's properties.
- Each generated standard multivariate normal vector is compared with the specification limit vector. Any generated vector out of the specification limits is recorded as nonconforming. Consequently, the total nonconforming vectors are divided by

the sample size at the end of the generation process to estimate the percentage of nonconforming (PNC) samples as in Equation (2) [6]:

- Each sample of the generated data is compared against the corresponding specification limit vector. The samples that fall outside the specification limits are considered nonconforming; then, the percentage of nonconforming (PNC) is estimated using the following equation [58]:

$$PNC = \frac{Number\ of\ nonconforming\ vectors}{Sample\ size} \quad (6)$$

- The multivariate capability index is then estimated using the following formula [59]:

$$C_p \frac{\varphi^{-1}(0.5 + 0.5(1 - PNC))}{3} \quad (7)$$

5. Research Results

5.1. Establishing Specification Limits

Table 2 provides a detailed reference for assessing the dimensional accuracy of various QC in AM processes based on the ISO 2768 standard. It includes nominal dimensions for features such as pin diameters, hole diameters, and lateral features (LFs), along with upper and lower specification limits (USL and LSL) categorized into four tolerance levels: Fine, Medium, Coarse, and Very Coarse. These tolerance classifications help determine the acceptable variation for each feature, with Fine tolerances allowing minimal deviation and Very Coarse tolerances permitting the largest deviations. By comparing measured dimensions of manufactured parts against these predefined limits, Table 2 shows specification limits according to the ISO 2768 standard, which facilitates process capability evaluation, quality control, and deviation analysis. For instance, a pin diameter with a nominal dimension of 4 mm can have an allowable range of 3.95 mm to 4.05 mm under Fine tolerance, while the range expands to 3.5 mm to 4.5 mm under Very Coarse tolerance. This differentiation directly affects process selection—high-precision processes such as SLA and EBM can meet Fine or Medium tolerances, whereas FDM generally meets only Coarse or Very Coarse tolerances. Consequently, the table serves as a vital tool for optimizing process parameters, ensuring compliance with industry standards, and determining the suitability of AM technologies for precision manufacturing applications.

After determining the sample mean and standard deviation for each dimension, the natural specification limits were computed for the three AM processes. A representative subset of results is illustrated in Table 3. The results revealed differences in both centering (process mean) and spread (process standard deviation) between the EBM, FDM, and SLA processes. EBM generally exhibits lower standard deviations for features such as Pin Diameter X (σ = 0.03) and LF Hole Diameter (σ = 0.03), indicating tighter local process control for these dimensions. At the same time, certain EBM features (e.g., Hole Diameters X and Y) reveal larger standard deviations (0.05), implying variability that may be attributable to thermal gradients or build parameters specific to EBM. For FDM, the process means for Pin Diameter X (4.00) and Y (4.02) lie near the midpoint of the calculated tolerance limits, yet the higher standard deviation (0.05) for Pin Diameter X suggests greater fluctuation in material deposition consistency. Moreover, the observed standard deviations of 0.04 for Hole Diameters X and Y suggest that, while still relatively controlled, FDM may require more frequent calibration or optimized extrusion settings to further reduce dimensional scatter. The SLA process demonstrates intermediate values in terms of mean and spread, with Pin Diameter X (mean 4.02, σ = 0.03) well centered, whereas Pin Diameter Y shows a slightly higher standard deviation (0.05). These results may be linked to variations in resin flow or curing consistency, which can differentially affect geometric features. Importantly,

all three processes generally remain within their defined tolerance bands—particularly for lower-dimensional features like the LF Hole Diameter and LF Square Width—which implies that, under stable conditions, each method is capable of producing parts that meet basic dimensional requirements. Identifying which features drive variability (e.g., Hole Diameter in EBM, Pin Diameter in FDM, Pin Diameter Y in SLA) highlights where each process requires calibration or compensation. By examining the interplay of mean centering and standard deviation against the tolerance ranges, this analysis illuminates areas of robust control, as well as potential opportunities for refining machine parameters, material handling, and environmental conditions to achieve more uniform part quality.

Table 2. Nominal dimensions and specification limits according to the ISO 2768 standard.

QC	Nominal Dimensions	Specification Limits According to ISO 2768 Standard							
		Fine Limits		Medium Limits		Coarse Limits		Very Coarse Limits	
		USL	LSL	USL	LSL	USL	LSL	USL	LSL
Pin Diameter X (QC1)	4	4.05	3.95	4.1	3.9	4.3	3.7	4.5	3.5
Pin Diameter Y (QC2)	4	4.05	3.95	4.1	3.9	4.3	3.7	4.5	3.5
Hole Diameter X (QC3)	4	4.05	3.95	4.1	3.9	4.3	3.7	4.5	3.5
Hole Diameter Y (QC4)	4	4.05	3.95	4.1	3.9	4.3	3.7	4.5	3.5
LF Hole Diameter (QC5)	3	3.05	2.95	3.1	2.9	3.3	2.7	3.5	2.5
LF Square Width (QC6)	3	3.05	2.95	3.1	2.9	3.3	2.7	3.5	2.5
LF Square Height (QC7)	3	3.05	2.95	3.1	2.9	3.3	2.7	3.5	2.5

Table 3. Natural specification limits for EBM, FDM, and SLA AM processes.

QC	EBM				FDM				SLA			
	Natural Limits		Process Mean	Process STD	Natural Limits		Process Mean	Process STD	Natural Limits		Process Mean	Process STD
	USL	LSL			USL	LSL			USL	LSL		
QC1	4.18	3.98	4.08	0.03	4.14	3.86	4.00	0.05	4.10	3.94	4.02	0.03
QC2	4.22	3.94	4.08	0.05	4.14	3.89	4.02	0.04	4.22	3.93	4.08	0.05
QC3	4.10	3.80	3.95	0.05	4.08	3.86	3.97	0.04	3.98	3.72	3.85	0.04
QC4	4.05	3.75	3.90	0.05	4.06	3.79	3.93	0.04	3.98	3.72	3.85	0.04
QC5	3.07	2.91	2.99	0.03	2.94	2.77	2.85	0.03	2.89	2.73	2.81	0.03
QC6	2.91	2.71	2.81	0.03	3.01	2.82	2.91	0.03	2.90	2.71	2.80	0.03
QC7	3.28	3.10	3.19	0.03	3.00	2.84	2.92	0.03	3.28	3.12	3.20	0.03

5.2. Normality Assumption and Correlation

To reduce skewness and improve normality, a root transformation was applied to the dimensional characteristics. The transformation follows a skewness-based search algorithm that evaluates fractional powers between 0 and 1 and selects the exponent that minimizes the absolute value of the sample skewness for each variable. After transformation, univariate and Mardia's multivariate skewness diagnostics indicated improved adherence to the normality assumption required for MEWMA monitoring and MPCI evaluation, as shown in Table 4.

Table 4. Skewness for original and transformed data.

Process	Variable	Original Data	Transformed Data	Improved Transformation	Mardia's Multivariate Skewness
EBM	Pin Diameter X (QC1)	0.184	0.359	−0.036	Mardia skewness statistic = 69.244 *p*-value = 0.877
	Pin Diameter Y (QC2)	0.085	–	–	
	Hole Diameter X (QC3)	0.291	0.135	0.054	
	Hole Diameter Y (QC4)	−0.025	–	–	
	LF Hole Diameter (QC5)	0.147	0.114	−0.029	
	LF Square Width (QC6)	0.105	−0.770	−0.018	
	LF Square Height (QC7)	0.575	0.751	−0.028	
FDM	Pin Diameter X (QC1)	−0.517	−0.348	−0.081	Mardia skewness statistic = 47.210 *p*-value = 0.999
	Pin Diameter Y (QC2)	−0.071	–	–	
	Hole Diameter X (QC3)	−0.085	–	–	
	Hole Diameter Y (QC4)	−0.088	–	–	
	LF Hole Diameter (QC5)	−0.269	−0.608	−0.056	
	LF Square Width (QC6)	0.282	0.111	0.061	
	LF Square Height (QC7)	−0.499	−0.532	−0.246	
SLA	Pin Diameter X (QC1)	0.041	–	0.071	Mardia skewness statistic = 74.764 *p*-value = 0.754
	Pin Diameter Y (QC2)	−0.082	–	–	
	Hole Diameter X (QC3)	−0.693	−0.376	−0.039	
	Hole Diameter Y (QC4)	−0.205	−0.447	−0.116	
	LF Hole Diameter (QC5)	−0.704	−1.057	–	
	LF Square Width (QC6)	0.166	−0.284	−0.052	
	LF Square Height (QC7)	−0.204	0.407	−0.028	

Table 4 presents skewness values in the three AM processes—EBM, FDM, and SLA—progress from the skewness of original data to the transformed data and, ultimately, the improved transformation. In general, positive skewness values (e.g., EBM Pin Diameter X at 0.184) indicate right-skewed distributions with heavier right tails, whereas negative skewness values (e.g., FDM Pin Diameter X at −0.517) suggest left-skewed distributions with heavier left tails. Across the original data, one observes a mix of both positive and negative skewness, implying that some features are skewed to the right (e.g., EBM Hole Diameter X at 0.291), while others are skewed to the left (e.g., SLA Hole Diameter X at −0.693). This variability underscores the heterogeneous nature of dimensional deviations in AM processes, where factors such as layer thickness, thermal fluctuations, and material flow can yield non-symmetric distributions.

By comparing the transformed data to the original data, one can see that many skewness values move closer to zero, suggesting that transformations (possibly Box–Cox, log, or other families) are effectively reducing the tail weight in at least one direction. For instance, EBM LF Square Width shifts from a moderately positive skew of 0.105 to −0.770, signifying a swing toward negative skew. Although this indicates a substantial change in distribution shape, the highly negative value after transformation may reflect overcorrection. In the "Improved Transformation" column, refinements appear to mitigate excessive shifts. For example, that same LF Square Width value rises to −0.018, which is near zero and suggests a more symmetric distribution. Similar corrective patterns appear for FDM Hole Diameter

X (from −0.085 originally to −0.608, then finally to −0.056) and SLA LF Hole Diameter (−0.704, −1.057, −0.052), highlighting the iterative nature of transformation selection to achieve near-zero skewness. Overall, these improved transformations demonstrate the importance of tailoring the choice and parameters of skewness-reducing procedures to each data set, as a single global approach may not uniformly account for the different degrees and directions of skew encountered in complex additive manufacturing processes.

The correlation matrices for the seven dimensional characteristics (Table 5) reveal process-dependent correlation structures. For EBM, moderate positive correlations were observed among features belonging to the same geometric group, such as hole diameters and square features, whereas cross-feature correlations were generally weak. FDM exhibited a tendency toward negative correlations, particularly between large-feature dimensions. SLA showed a mixture of moderate positive and negative correlations.

Table 5. The correlation matrices.

EBM	**QC1**	**QC2**	**QC3**	**QC4**	**QC5**	**QC6**
QC2	0.138					
QC3	−0.052	0.083				
QC4	−0.257	0.163	0.298			
QC5	−0.038	0.259	0.422	0.252		
QC6	0.372	0.206	−0.017	0.057	−0.027	
QC7	0.097	−0.062	−0.141	0.184	−0.069	−0.184
FDM	QC1	QC2	QC3	QC4	QC5	QC6
QC2	−0.034					
QC3	0.095	−0.099				
QC4	−0.051	−0.048	0.01			
QC5	−0.333	−0.17	−0.129	0.065		
QC6	0.235	−0.014	−0.141	−0.139	0.145	
QC7	−0.056	0.214	−0.317	−0.037	0.048	0.042
SLA	QC1	QC2	QC3	QC4	QC5	QC6
QC2	0.039					
QC3	0.114	−0.277				
QC4	0.007	−0.001	0.301			
QC5	−0.316	0	0.252	0.013		
QC6	−0.167	0.018	0.111	−0.392	0.469	
QC7	−0.161	0.022	−0.087	−0.313	0.154	0.238

5.3. Process Monitoring Results

Table 6 presents different optimized parameters of the Multivariate Exponentially Weighted Moving Average (MEWMA) control chart, specifically the Lambda (λ), control limit (h_4), and *ARL* for different AM processes (EBM, FDM, and SLA). The objective was to optimize the control chart parameters to achieve an *ARL* of 370, which represents the expected number of observations before a false alarm is triggered. From this table, we can analyze how different parameter combinations impact *ARL*. For EBM, the highest ARL achieved was 382 (λ = 0.844, h_4 = 2.888), while other values were significantly lower. In the FDM process, ARL values varied widely, with the highest being 352 (λ = 0.362, h_4 = 2.996) and the lowest standing at 136 (λ = 0.479, h_4 = 2.973), indicating that FDM is more sensitive

to parameter selection. For SLA, the ARL values are closer to the target, with 367 (λ = 0.742, h_4 = 2.94) and 361 (λ = 0.532, h_4 = 2.999) being the closest to 370. To achieve the desired *ARL* = 370, the optimal parameter selection would likely be within the SLA process range, as its values are the closest to the target. Fine-tuning λ and h_4 within 0.65–0.75 for λ and 2.94–2.99 for h_4 could help stabilize *ARL* at 370. Further experimentation or interpolation between values may be necessary for precise optimization.

Table 6. Different optimized parameters of the Multivariate Exponentially Weighted Moving Average for EBM, FDM, and SLA.

Process	Lambda	h_4	ARL
EBM	0.217	2.974	216
	0.844	2.888	382
	0.342	2.996	201
	0.662	2.867	284
	0.545	2.842	312
FDM	0.362	2.996	352
	0.7	2.826	217
	0.479	2.973	136
	0.521	2.964	336
	0.678	2.785	244
SLA	0.742	2.94	367
	0.639	2.972	335
	0.532	2.999	361
	0.667	2.949	288
	0.46	2.995	384

Because the search was performed over a discrete grid of candidate (h_4 and λ) values, the resulting in-control *ARL* values did not always equal 370 exactly; some combinations produced *ARLs* slightly below (e.g., ≈352) or above (e.g., ≈384) the target. Parameter pairs were selected when the *ARL* lay within a narrow tolerance band around 370, which is acceptable given the Monte Carlo variability and has a negligible impact on the comparative performance of the charts. Interpolating (h_4 and λ) to match 370 exactly would not materially change the conclusions but would significantly increase computational effort.

The MEWMA control charts for the three additive manufacturing processes—EBM, FDM, and SLA—in Figure 8 illustrate the stability of each process over a series of sample numbers. The optimal parameters were selected based on the standard criterion of choosing the combination whose ARL is closest to 370. The selected pairs were EBM (λ = 0.844, h_4 = 2.888), FDM (λ = 0.362, h_4 = 2.996), and SLA (λ = 0.742, h_4 = 2.94). In all three charts, the data initially increases before reaching a steady state, indicating a period of adjustment before stabilization. The control limits, represented by the red dashed lines, remain constant and provide a threshold for detecting deviations. The EBM process exhibits the highest process values, while SLA stabilizes the fastest, suggesting a more consistent performance with lower fluctuations. FDM follows a similar trend, gradually leveling off within the control range. Importantly, none of the processes exceed the control limits, signifying that they are all operating within acceptable boundaries. This confirms that the chosen MEWMA parameters effectively monitor process stability. However, further refinement of

the λ and h_4 values may be necessary to achieve an ARL closer to the target of 370, ensuring optimal sensitivity and detection capability in the control system.

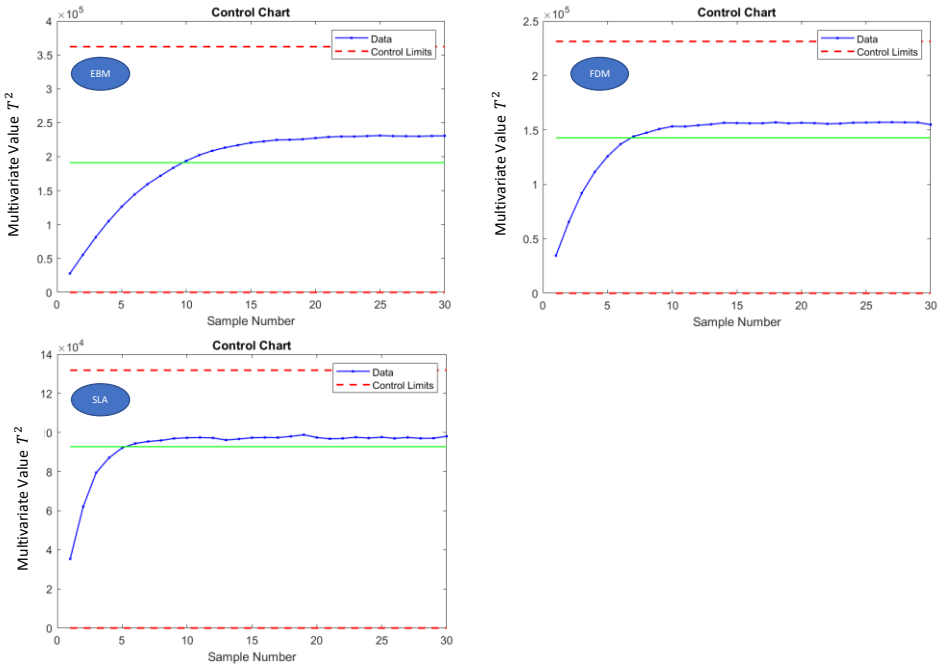


Figure 8. MEWMA control charts for additive manufacturing processes—EBM, FDM, and SLA.

5.4. Process Evaluation Results

The MPCIs for the three AM processes (EBM, FDM, and SLA) under different specification designations are presented in Table 7. The MPCIs are categorized based on Fine, Medium, Coarse, and Natural limits, providing insight into the capability of each process to meet varying levels of tolerance requirements. For Fine limits, all three processes exhibit an MPCI of 0.000, indicating that they do not meet the strictest specification requirements. Under Medium limits, only FDM shows a small capability index (0.005), while EBM and SLA remain at 0.000, suggesting limited adherence to moderate tolerances. In the category for Coarse limits, the MPCI values increase significantly, with FDM reaching 1.152, EBM reaching 0.888, and SLA reaching 0.916, indicating that the processes are more capable of meeting relaxed tolerances. In the second category of Coarse limits, the indices further increase, with EBM at 1.637, FDM at 1.575, and SLA at 1.268, reflecting a higher likelihood of meeting less stringent specifications. The Natural limits, which represent the inherent capability of each process without imposed specification constraints, show values of 0.759 for EBM, 0.782 for FDM, and 0.772 for SLA. These values suggest that FDM has the highest natural capability, followed closely by SLA and EBM. Overall, the results indicate that while none of the AM processes can reliably meet Fine and Medium tolerances, they are more suited for Coarse and Natural limit specifications, with FDM demonstrating the highest process capability across most categories.

Table 7. Multivariate Process Capability Indices (MPCIs) for additive manufacturing (AM) processes (EBM, FDM, and SLA).

Process	Fine Limits	Medium Limits	Coarse Limits	Very Coarse Limits	Natural Limits
EBM	0.000	0.000	0.888	1.637	0.759
FDM	0.000	0.005	1.152	1.575	0.782
SLA	0.000	0.000	0.916	1.268	0.772

6. Research Discussion

In this section, we discuss our analysis of the effect of changing the mean and variation of the considered processes on MPCIs. The resulting MPCI changes will be discussed, together with the descriptive statistics of each process. Relating sensitivity analysis results with process statistics brings insights into process improvements. Sensitivity analysis was applied to the EBM, FDM, and SLA processes by estimating MPCIs when changing the mean and/or standard deviation of each QC separately. This paper considered three AM processes; for each process with seven QCs, each QC underwent positive or negative changes regarding the mean, standard deviation, or both. Consequently, for our research, we conducted 126 tests to evaluate the effect of changing processes' mean and standard deviation on MPCI results (three process× seven QCs × six permutations of mean and standard deviation). The MPCIs were estimated during sensitivity analysis using the Coarse limits in Table 8.

Table 8 presents the mean, standard deviation, minimum datapoint, maximum datapoint, and skewness of each QC for the EBM, FDM, and SLA processes. The table was presented to first investigate the central tendency and the variation of the processes, and then relate these measures to the MPCI changes in Figure 9.

Table 8. Descriptive statistics of measured QCs for EBM, FDM, and SLA processes.

Process	Measure	Quality Characteristics						
		QC1	QC2	QC3	QC4	QC5	QC6	QC7
EBM	Mean	4.076	4.077	3.950	3.904	2.988	2.809	3.192
	STD	0.033	0.046	0.049	0.050	0.027	0.034	0.031
	Max	4.142	4.168	4.051	4.001	3.048	2.895	3.264
	Min	4.017	3.986	3.872	3.820	2.938	2.729	3.147
	Skew	0.193	0.090	0.307	−0.026	0.155	0.110	0.606
FDM	Mean	4.003	4.016	3.972	3.927	2.852	2.914	2.918
	STD	0.047	0.040	0.037	0.044	0.028	0.032	0.026
	Max	4.086	4.112	4.052	3.998	2.910	2.977	2.955
	Min	3.894	3.927	3.894	3.832	2.800	2.869	2.866
	Skew	−0.544	−0.075	−0.089	−0.093	−0.284	0.297	−0.525
SLA	Mean	4.021	4.076	3.853	3.847	2.810	2.803	3.202
	STD	0.026	0.047	0.044	0.043	0.026	0.032	0.027
	Max	4.067	4.187	3.927	3.919	2.854	2.868	3.254
	Min	3.978	3.968	3.732	3.754	2.743	2.743	3.147
	Skew	0.043	−0.086	−0.730	−0.216	−0.742	0.174	−0.215
USL		4.300	4.300	4.300	4.300	3.300	3.300	3.300
LSL		3.700	3.700	3.700	3.700	2.700	2.700	2.700
Nominal Dimension		4	4	4	4	3	3	3

Table 8 shows that the mean of the EBM QCs (the name of each QC is mentioned in Table 4) is fluctuating above and under the nominal dimension. The first QC of the EBM produced part shows stable performance, as its mean is relatively near to the nominal value, and there is only small variation. The MPCI results shown in Figure 9 indicate that changing the mean and standard deviation of QC1 always improves the MPCI results. This is a random process that may occur due to the stability of QC1. However, increasing the mean of QC2 dropped the MPCI to zero. This is due to the fact that the actual mean of QC2 is above the nominal, and the standard deviation is higher than that of QC1. It is worth noting that changing the standard deviation of all EBM QCs improves the MPCI. Regarding the FDM process, increasing the process mean will dramatically decrease the

MPCI results, especially for QC2, QC3, and QC4. Finally, most of the mean and standard deviation changes adversely affect the MPCIs.

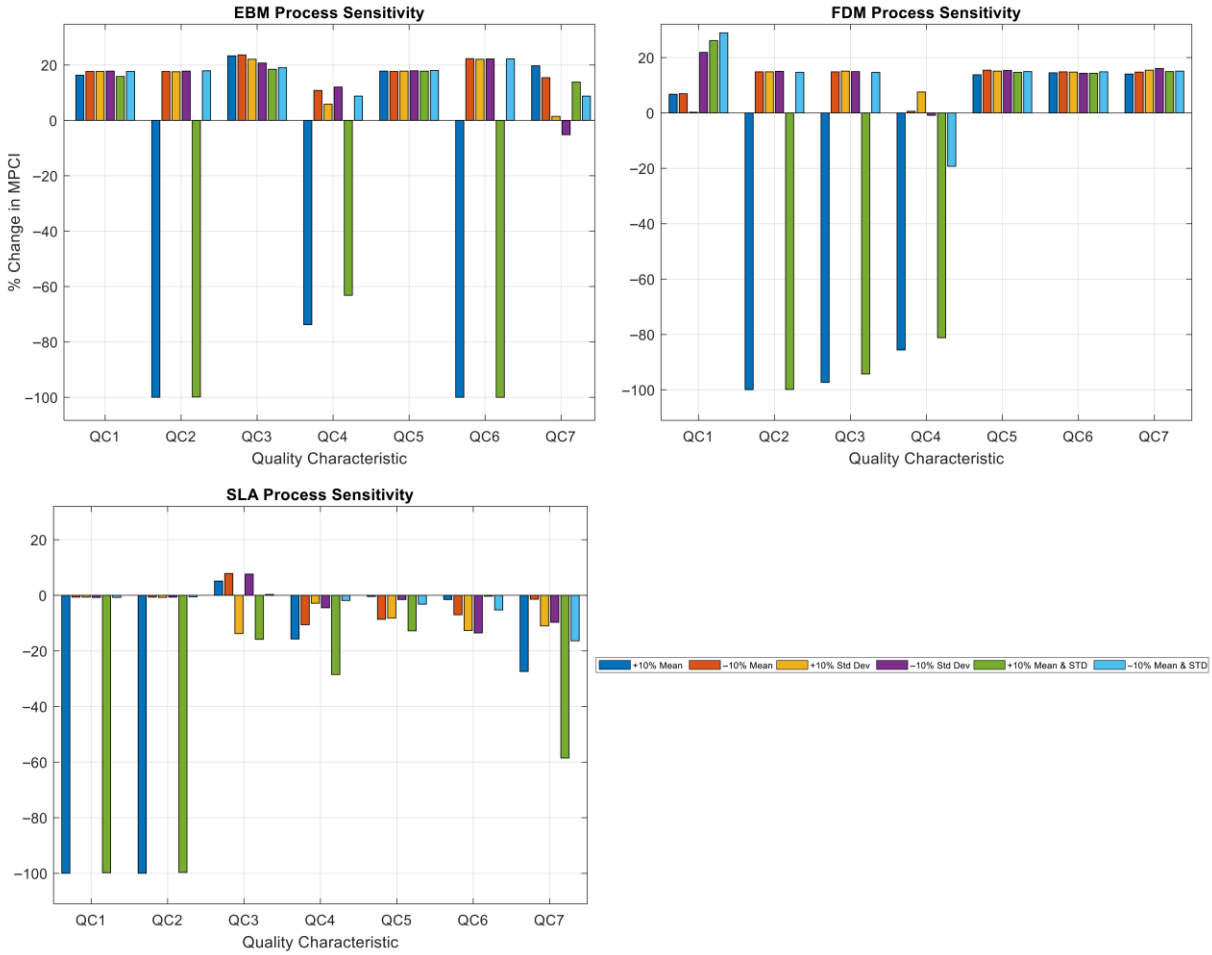


Figure 9. MPCI values under 10% changes in mean and/or standard deviation.

The results have several practical implications for AM quality engineering. First, the distinct multivariate variability structures observed across EBM, FDM, and SLA indicate that process selection should not only consider average dimensional accuracy but also the joint behavior of multiple features. Second, the dependence of capability on tolerance class provides guidance for tolerance specification—certain processes remain stable when tolerances are tightened, while others exhibit sharp capability reductions. This information helps avoid over-specification and unnecessary manufacturing costs. Third, the correlation structure highlights which geometric features are most sensitive to each process. Finally, the MEWMA-based monitoring framework demonstrated here can be integrated into AM production to detect deviations in real time once Phase-I baselines are established. Overall, the results support more informed decision-making in AM process selection, tolerance assignment, and quality control planning.

7. Research Conclusions

The research goal was to monitor, evaluate, and compare selected AM processes—EMB, FDM, and SLA processes—in terms of capability and process variation. That multivariate analysis was used in this study to model variation and estimate AM processes' capability to ensure that correlated QCs of the same product are optimally modeled. The normality tests showed that most of the QC data are not normally distributed. Across the original data, one observes a mix of both positive and negative skewness, implying that some features

are skewed to the right (e.g., EBM Hole Diameter X at 0.291), while others are skewed to the left (e.g., SLA Hole Diameter X at −0.693).

Using a MEWMA control chart, the investigated AM processes showed consistent patterns in terms of process variation. The objective was to optimize the control chart parameters. For EBM, the highest ARL achieved was 382 (λ = 0.844, h_4 = 2.888), while other values were significantly lower. In the FDM process, ARL values varied widely, with the highest being 352 (λ = 0.362, h_4 = 2.996) and the lowest standing at 136 (λ = 0.479, h_4 = 2.973), indicating that FDM is more sensitive to parameter selection. For SLA, the ARL values are closer to the target, with 367 (λ = 0.742, h_4 = 2.94) and 361 (λ = 0.532, h_4 = 2.999) being the closest to 370. Despite the fact that the processes were stable, it was observed that their means were not centered.

The MPCI results clearly show that the process means are off-center. According to MPCI's findings, all of the processes under investigation are unable to produce parts that fall within both the natural tolerance limits and the fine and medium ISO specification limits. Additionally, only the FDM process demonstrated the ability to produce parts that fell within the coarse parameters of ISO specifications. However, all of the processes that were taken into consideration were able to produce parts within Very Coarse limits. To model the effect of process centering and process variation on the process capability indices, sensitivity analysis was conducted by changing the process mean and standard deviation. Sensitivity analysis results proved that most of QCs are very sensitive to the changes in mean and standard deviation.

However, the study is limited to a specific polymer material and process parameters. Extending the analysis to other materials, geometries, and AM technologies would enhance the model's findings. Additionally, incorporating other multivariate and intelligent optimization techniques—such as machine learning or adaptive control—could further improve process prediction. From an industrial perspective, the proposed methodology offers a practical framework for manufacturers to evaluate AM processes more systematically. Further research work could focus on the monitoring and evaluation of AM processes, considering various AM processes, materials, parts, and process parameters. An effective strategy for improving AM processes is real-time monitoring.

Supplementary Materials: The following supporting information can be downloaded at: https://www.mdpi.com/article/10.3390/pr13123825/s1.

Author Contributions: Conceptualization, A.M.A.-A., M.A. and W.A.; Methodology, A.M.A.-A. and M.A.; Software, M.A. and W.A.; Validation, M.A.; Formal analysis, M.A.; Investigation, M.A.; Resources, A.M.A.-A., M.A. and W.A.; Data curation, M.A.; Writing—original draft, M.A. and W.A.; Writing—review & editing, A.M.A.-A., M.A. and W.A.; Visualization, M.A.; Supervision, A.M.A.-A.; Project administration, A.M.A.-A.; Funding acquisition, A.M.A.-A. All authors have read and agreed to the published version of the manuscript.

Funding: This study received funding from the Raytheon Chair for Systems Engineering. The authors are grateful to the Raytheon Chair for Systems Engineering for funding.

Data Availability Statement: The original contributions of this study are included in the article/Supplementary Materials. Further inquiries can be directed to the corresponding author.

Conflicts of Interest: The authors declare no conflicts of interest.

References

1. Dabwan, A.; Anwar, S.; Al-Samhan, A.M.; Alqahtani, K.N.; Nasr, M.M.; Kaid, H.; Ameen, W. CNC turning of an additively manufactured complex profile Ti6Al4V component considering the effect of layer orientations. *Processes* **2023**, *11*, 1031. [CrossRef]
2. Kumar, S.; Tiwari, P.; Koloor, S.S.R. Mechanical, Morphological, and Electrical Characteristics of Cu-Loaded Acrylic Paint on a Fused Deposition Modeling Printed Polylactic Acid Surface. *Processes* **2025**, *13*, 1059. [CrossRef]

3. Gibson, I.; Rosen, D.; Stucker, B.; Khorasani, M. Development of additive manufacturing technology. In *Additive Manufacturing Technologies*; Springer: Berlin/Heidelberg, Germany, 2021; pp. 23–51.
4. Kim, H.; Lin, Y.; Tseng, T.-L.B. A review on quality control in additive manufacturing. *Rapid Prototyp. J.* **2018**, *24*, 645–669. [CrossRef]
5. Alatefi, M.; Ahmad, S.; Alkahtani, M. Performance evaluation using multivariate non-normal process capability. *Processes* **2019**, *7*, 833. [CrossRef]
6. Montgomery, D.C. *Introduction to Statistical Quality Control*; John Wiley & Sons: Hoboken, NJ, USA, 2020.
7. Grigoriev, S.; Nikitin, N.; Yanushevich, O.; Krikheli, N.; Khmyrov, R.; Strunevich, D.; Soloninkin, M.; Pinargote, N.W.S.; Peretyagin, P.; Smirnov, A. Mechanical properties variation of samples fabricated by fused deposition additive manufacturing as a function of filler percentage and structure for different plastics. *Sci. Rep.* **2024**, *14*, 28344. [CrossRef] [PubMed]
8. Alatefi, M.; Al-Ahmari, A.M.; AlFaify, A.Y.; Saleh, M. A framework for multivariate statistical quality monitoring of additive manufacturing: Fused filament fabrication process. *Processes* **2023**, *11*, 1216. [CrossRef]
9. Daghrery, A.; Vinothkumar, T.S.; Majrashi, H.; Faqihi, G.; Gofshi, R.; Almasoudi, S.; Madkhali, R.; Lam, W.Y.H.; Lunkad, H.; Chourasia, H.; et al. Dimensional accuracy of additive and subtractive manufactured ceramic-reinforced hybrid composite inlays: A CBCT-based in vitro study. *Sci. Rep.* **2025**, *15*, 6048. [CrossRef] [PubMed]
10. Baig, S.; Jam, A.; Beretta, S.; Shao, S.; Shamsaei, N. Non-destructive detection of critical defects in additive manufacturing. *Sci. Rep.* **2025**, *15*, 6740. [CrossRef]
11. Peng, L.; Benavidez, E.; Mukherjee, S.; Morales, R.E.; Tringe, J.W.; Stobbe, D.; Deng, Y. In-situ 3D temperature field modeling and characterization using eddy current for metal additive manufacturing process monitoring. *Sci. Rep.* **2025**, *15*, 9999. [CrossRef]
12. Alatefi, M.; Al-Ahmari, A.M.; AlFaify, A.Y.; Saleh, M. A framework for fused deposition modelling process evaluation using multivariate process capability analysis. *PLoS ONE* **2024**, *19*, e0308380. [CrossRef] [PubMed]
13. Gupta, A.; Rao, P.S.; Mittal, K. 3D technology printing: A review. In *Challenges and Opportunities in Industrial and Mechanical Engineering: A Progressive Research Outlook*; CRC Press: Boca Raton, FL, USA, 2024; pp. 866–883.
14. Srivastava, M.; Rathee, S. Additive manufacturing: Recent trends, applications and future outlooks. *Prog. Addit. Manuf.* **2022**, *7*, 261–287. [CrossRef]
15. Ghinea, M.; Niculescu, A.C.; Rosca, B.D. Enhancing FDM Rapid Prototyping for Industry 4.0 Applications through Simulation and Optimisation Techniques. *Materials* **2025**, *18*, 4555. [CrossRef]
16. Ramsperger, M.; Eichler, S. Electron beam based additive manufacturing of alloy 247 for turbine engine application: From research towards industrialization. *Metall. Mater. Trans. A* **2023**, *54*, 1730–1743. [CrossRef]
17. Ahmad, M.; Javaid, M.; Haleem, A. A study on fused deposition modeling (FDM) and laser-based additive manufacturing (LBAM) in the medical field. *Intell. Pharm.* **2024**, *2*, 381–391. [CrossRef]
18. Abbasi, M.; Váz, P.; Silva, J.; Martins, P. Head-to-Head evaluation of FDM and SLA in additive manufacturing: Performance, cost, and environmental perspectives. *Appl. Sci.* **2025**, *15*, 2245. [CrossRef]
19. Zhou, H.-R.; Yang, H.; Li, H.-Q.; Ma, Y.-C.; Yu, S.; Shi, J.; Cheng, J.-C.; Gao, P.; Yu, B.; Miao, Z.-Q.; et al. Advancements in machine learning for material design and process optimization in the field of additive manufacturing. *China Foundry* **2024**, *21*, 101–115. [CrossRef]
20. Gradl, P.; Tinker, D.C.; Park, A.; Mireles, O.R.; Garcia, M.; Wilkerson, R.; Mckinney, C. Robust metal additive manufacturing process selection and development for aerospace components. *J. Mater. Eng. Perform.* **2022**, *31*, 6013–6044. [CrossRef]
21. Ameen, W.; Mohammed, M.K.; Al-Ahmari, A. Evaluation of support structure removability for additively manufactured Ti6Al4V overhangs via electron beam melting. *Metals* **2019**, *9*, 1211. [CrossRef]
22. Ameen, W.; Al-Ahmari, A.; Mohammed, M.K.; Mian, S.H. Manufacturability of overhanging holes using electron beam melting. *Metals* **2018**, *8*, 397. [CrossRef]
23. Murr, L.; Gaytan, S.; Ceylan, A.; Martinez, E.; Martinez, J.; Hernandez, D.; Machado, B.; Ramirez, D.; Medina, F.; Collins, S.; et al. Characterization of titanium aluminide alloy components fabricated by additive manufacturing using electron beam melting. *Acta Mater.* **2010**, *58*, 1887–1894. [CrossRef]
24. Ameen, W.; Al-Ahmari, A.; Mian, S.H.; Mohammed, M.K.; Kaid, H.; Abdulhameed, O. Optimization of tree-like support for titanium overhang structures produced via electron beam melting. *Sustainability* **2022**, *14*, 13017. [CrossRef]
25. Ameen, W.; Alatefi, M.; Al-Ahmari, A.; Aldoukhi, M.; Ghaleb, A.M.; Alfaify, A.Y. Multivariate process capability analysis for evaluating metal additive manufacturing via electron beam melting. *Mater. Res. Express* **2024**, *11*, 096516. [CrossRef]
26. Lee, J.; Park, H.J.; Chai, S.; Kim, G.R.; Yong, H.; Bae, S.J.; Kwon, D. Review on Quality Control Methods in Metal Additive Manufacturing. *Appl. Sci.* **2021**, *11*, 1966. [CrossRef]
27. Edwards, P.; O'COnner, A.; Ramulu, M. Electron beam additive manufacturing of titanium components: Properties and performance. *J. Manuf. Sci. Eng.* **2013**, *135*, 061016. [CrossRef]

28. García-Hernández, C.; García-Cabezón, C.; González-Diez, F.; Ampudia, M.; Juanes-Gusano, D.; Rodriguez-Cabello, J.C.; Martín-Pedrosa, F. Effect of processing on microstructure, mechanical properties, corrosion and biocompatibility of additive manufacturing Ti-6Al-4V orthopaedic implants. *Sci. Rep.* **2025**, *15*, 14087. [CrossRef]
29. Moazzen, P.; Shahriari, A.; Shamsdini, S.; Seraj, P.; Forooghi, F.; Aghayar, Y.; Shakerin, S.; Purdy, M.R.; Mohammadi, M. Optimum corrosion performance using microstructure design and additive manufacturing process control. *npj Mater. Degrad.* **2025**, *9*, 10. [CrossRef]
30. Tientcheu, S.W.T.; Djouda, J.M.; Bouaziz, M.A.; Lacazedieu, E. A review on fused deposition modeling materials with analysis of key process parameters influence on mechanical properties. *Int. J. Adv. Manuf. Technol.* **2024**, *130*, 2119–2158. [CrossRef]
31. Turner, B.N.; Strong, R.; Gold, S.A. A review of melt extrusion additive manufacturing processes: I. Process design and modeling. *Rapid Prototyp. J.* **2014**, *20*, 192–204. [CrossRef]
32. Bellini, A.; Guceri, S.; Bertoldi, M. Liquefier dynamics in fused deposition. *J. Manuf. Sci. Eng.* **2004**, *126*, 237–246. [CrossRef]
33. Agarwala, M.K.; Jamalabad, V.R.; Langrana, N.A.; Safari, A.; Whalen, P.J.; Danforth, S.C. Structural quality of parts processed by fused deposition. *Rapid Prototyp. J.* **1996**, *2*, 4–19. [CrossRef]
34. Idà, E.; Nanetti, F.; Mottola, G. An Alternative Parallel Mechanism for Horizontal Positioning of a Nozzle in an FDM 3D Printer. *Machines* **2022**, *10*, 542. [CrossRef]
35. Gardan, J. Additive manufacturing technologies: State of the art and trends. In *Additive Manufacturing Handbook*; CRC Press: Boca Raton, FL, USA, 2017; pp. 149–168.
36. Lewiński, T.; Kukiełka, K.; Chaciński, T.; Jaskólski, P. Effect of parameters of the stereolithography process on the part quality. *J. Mech. Energy Eng.* **2022**, *6*, 1–12. [CrossRef]
37. Huang, J.; Qin, Q.; Wang, J. A review of stereolithography: Processes and systems. *Processes* **2020**, *8*, 1138. [CrossRef]
38. Campanelli, S.; Cardano, G.; Giannoccaro, R.; Ludovico, A.; Bohez, E. Statistical analysis of the stereolithographic process to improve the accuracy. *Comput. Aided Des.* **2007**, *39*, 80–86. [CrossRef]
39. Udroiu, R.; Braga, I.C. System performance and process capability in additive manufacturing: Quality control for polymer jetting. *Polymers* **2020**, *12*, 1292. [CrossRef]
40. Zhao, J.; Yang, Y.; Li, L. A comprehensive evaluation for different post-curing methods used in stereolithography additive manufacturing. *J. Manuf. Process.* **2020**, *56*, 867–877. [CrossRef]
41. Zhou, J.G.; Herscovici, D.; Chen, C.C. Parametric process optimization to improve the accuracy of rapid prototyped stereolithography parts. *Int. J. Mach. Tools Manuf.* **2000**, *40*, 363–379. [CrossRef]
42. Weheba, G.; Sanchez-Marsa, A. Using response surface methodology to optimize the stereolithography process. *Rapid Prototyp. J.* **2006**, *12*, 72–77. [CrossRef]
43. Mhmood, T.R.; Al-Karkhi, N.K. Multiobjective optimization of stereolithography for dental bridge based on a simple shape model using Taguchi and response surface methods. *Appl. Sci.* **2023**, *13*, 10911. [CrossRef]
44. Kadauw, A.A.A. Neural Network Optimization of Mechanical Properties of ABS-like Photopolymer Utilizing Stereolithography (SLA) 3D Printing. *J. Manuf. Mater. Process.* **2025**, *9*, 116. [CrossRef]
45. Basar, G.; Der, O.; Guvenc, M.A. AI-powered hybrid metaheuristic optimization for predicting surface roughness and kerf width in CO_2 laser cutting of 3D-printed PLA-CF composites. *J. Thermoplast. Compos. Mater.* **2025**, *38*, 08927057251344183. [CrossRef]
46. Valino, A.D.; Dizon, J.R.C.; Espera, A.H., Jr.; Chen, Q.; Messman, J.; Advincula, R.C. Advances in 3D printing of thermoplastic polymer composites and nanocomposites. *Prog. Polym. Sci.* **2019**, *98*, 101162. [CrossRef]
47. Zhou, L.; Miller, J.; Vezza, J.; Mayster, M.; Raffay, M.; Justice, Q.; Tamimi, Z.A.; Hansotte, G.; Sunkara, L.D.; Bernat, J. Additive manufacturing: A comprehensive review. *Sensors* **2024**, *24*, 2668. [CrossRef]
48. Goh, G.D.; Wong, K.K.; Tan, N.; Seet, H.L.; Nai, M.L.S. Large-format additive manufacturing of polymers: A review of fabrication processes, materials, and design. *Virtual Phys. Prototyp.* **2024**, *19*, e2336160. [CrossRef]
49. Pepelnjak, T.; Stojšić, J.; Sevšek, L.; Movrin, D.; Milutinović, M. Influence of process parameters on the characteristics of additively manufactured parts made from advanced biopolymers. *Polymers* **2023**, *15*, 716. [CrossRef] [PubMed]
50. Jemghili, R.; Taleb, A.A.; Mansouri, K. Additive manufacturing technology, process parameters influencing product quality and its applications. *Int. J. Adv. Technol. Eng. Explor.* **2022**, *9*, 1678. [CrossRef]
51. Milutinović, B.; Đekić, P.; Pavlović, M.; Ristić, M.; Jović, G. Comparative analysis of 3D printing technologies (FDM and SLA) for the production of complex geometry parts. In Proceedings of the 23rd International Symposium INFOTEH-JAHORINA, Jahorina, East Sarajevo, Bosnia and Herzegovina, 20–22 March 2024.
52. Pereira, A.G.; Barbosa, G.F.; Filho, M.G.; Shiki, S.B.; da Silva, A.L. Quality Control in Extrusion-Based Additive Manufacturing: A Review of Machine Learning Approaches. *IEEE Trans. Cybern.* **2025**, *55*, 2522–2534. [CrossRef] [PubMed]
53. Choudhari, A.; Elder, J.; Mugale, M.; Karki, S.; Digole, S.; Omeike, S.; Borkar, T. Enhancing Quality Control: Image-Based Quantification of Carbides and Defect Remediation in Binder Jetting Additive Manufacturing. *Materials* **2024**, *17*, 2174. [CrossRef]
54. Moylan, S.; Slotwinski, J.; Cooke, A.; Jurrens, K.; Donmez, M.A. An additive manufacturing test artifact. *J. Res. Natl. Inst. Stand. Technol.* **2014**, *119*, 429. [CrossRef] [PubMed]

55. *ISO 2768-1:1989*; General Tolerances—Part 1: Tolerances for Linear and Angular Dimensions Without Individual Tolerance Indications. International Organization for Standardization: Geneva, Switzerland, 2015.
56. Gibson, I.; Rosen, D.; Stucker, B.; Khorasani, M. *Additive Manufacturing Technologies*; Springer: Berlin/Heidelberg, Germany, 2021.
57. Lowry, C.A.; Woodall, W.H.; Champ, C.W.; Rigdon, S.E. A multivariate exponentially weighted moving average control chart. *Technometrics* **1992**, *34*, 46–53. [CrossRef]
58. Gunaratne, N.G.T.; Abdollahian, M.A.; Huda, S.; Yearwood, J. Exponentially weighted control charts to monitor multivariate process variability for high dimensions. *Int. J. Prod. Res.* **2017**, *55*, 4948–4962. [CrossRef]
59. Abbasi, B.; Akhavan Niaki, S.T. Estimating process capability indices of multivariate nonnormal processes. *Int. J. Adv. Manuf. Technol.* **2010**, *50*, 823–830. [CrossRef]

Disclaimer/Publisher's Note: The statements, opinions and data contained in all publications are solely those of the individual author(s) and contributor(s) and not of MDPI and/or the editor(s). MDPI and/or the editor(s) disclaim responsibility for any injury to people or property resulting from any ideas, methods, instructions or products referred to in the content.